Dentomaxillofacial Radiology (2022) 51, 20210036

birpublications.org/dmfr

RESEARCH ARTICLE

Correlation of dynamic contrast-enhanced bone perfusion with morphologic ultra-short echo time MR imaging in medication-related osteonecrosis of the jaw

[1,2]Paul Schumann, [2,3]Sarah Morgenroth, [2,3]Florian A Huber, [2,4]Niels J Rupp, [5]Filippo Del Grande and [2,3]Roman Guggenberger

[1]Department of Cranio-Maxillo-Facial and Oral Surgery, University Hospital Zurich, Zurich, Switzerland; [2]Faculty of Medicine, University of Zurich, Zurich, Switzerland; [3]Institute of Diagnostic and Interventional Radiology, University Hospital Zurich, Zurich, Switzerland; [4]Department of Pathology and Molecular Pathology, University Hospital Zurich, Zurich, Switzerland; [5]Istituto di imaging della Svizzera Italiana, Regional Hospital of Lugano, Via Tesserete 46, Lugano, Switzerland

Objectives: To investigate whether dynamic contrast-enhanced (DCE)-MR bone perfusion could serve as surrogate for morphologic ultra-short echo time (UTE) bone images and to correlate perfusion with morphologic hallmarks in histologically proven foci of medication-related osteonecrosis of the jaw (MRONJ).
Methods: Retrospective study including 20 patients with established diagnosis of MRONJ. Qualitative consensus assessment of predefined jaw regions by two radiologists was used as reference standard using Likert scale (0–3) for standard imaging hallmarks in MRONJ (osteolysis, sclerosis, periosteal thickening). DCE-MRI measurements performed in corresponding regions of the mandible were then correlated with qualitative scores. Regions were grouped into "non-affected" and "pathologic" based on binarized Likert scores of different imaging hallmarks (0–1 *vs* 2–3). DCE-MRI measurements among hallmarks were compared using Mann–Whitney-*U*-testing. ROC (receiver-operating-characteristic) analysis was performed for each of the perfusion parameters to assess diagnostic performance for identification of MRONJ using morphologic ratings as reference standard.
Results: Median perfusion measurements of "pathologic" regions in wash-in, peak enhancement intensity and integrated area under the curve are significantly higher than those of "non-affected" regions, irrespective of reference imaging hallmark ($p < 0.05$). No significant perfusion differences were found between "pathologic" regions with and without osteolysis ($p = 0.180$). ROC analysis showed fair diagnostic performance of DCE-MRI parameters for identification of MRONJ (AUC 0.626–0.727).
Conclusions: DCE bone perfusion parameters are significantly increased in MRONJ compared to non-affected regions, irrespective of osteolysis. Due to certain overlap DCE-MRI bone perfusion cannot serve as full surrogate for UTE bone imaging but may enhance reader confidence.
Dentomaxillofacial Radiology (2022) **51**, 20210036. doi: 10.1259/dmfr.20210036

Cite this article as: Schumann P, Morgenroth S, Huber FA, Rupp NJ, Del Grande F, Guggenberger R. Correlation of dynamic contrast-enhanced bone perfusion with morphologic ultra-short echo time MR imaging in medication-related osteonecrosis of the jaw. *Dentomaxillofac Radiol* 2022; **51**: 20210036.

Keywords: Bisphosphonate-Associated Osteonecrosis of the Jaw; Perfusion Weighted MRI; Drug-Related Side Effects and Adverse Reactions

Correspondence to: Florian A Huber, E-mail: florian.huber@usz.ch

Received 25 January 2021; revised 14 July 2021; accepted 01 August 2021
Paul Schumann and Sarah Morgenroth have contributed equally to this study and should be considered as co-first authors.

Introduction

According to the American Association of Oral and Maxillofacial Surgeons (AAOMS), medication related osteonecrosis of the jaw (MRONJ) is defined by visually exposed bone or bone-probing fistula in the maxillofacial region persisting for longer than 8 weeks, in patients with a history of antiresorptive therapy (ART) without prior radiation to the jaw.[1] MRONJ was first associated with bisphosphonates, but has now been linked to many antiresorptive and cancer drugs.[1] MRONJ primarily occurs in the alveolar bone of the jaw affecting the mandible more often than the maxilla (80% *vs* 20%).[1] The current pathogenetic concept for MRONJ is multifactorial and based in part on the accumulation of antiresorptive drugs in the jawbone[2,3] leading to bone-remodeling inhibition and eventual bone necrosis in response to inflammation of the periodontal space.[4]

The AAOMS initially proposed a 3-grade staging system (Grade 1–3), depending on clinical symptoms and degree of disease extent. In 2009, Stage 0 was added as the non-exposed variant of the disease, in order to include a significant proportion of patients on ART who do not show exposed jaw bone, but present with persistent non-specific symptoms (odontalgia, dull aching pain, sinus pain) and non-specific clinical findings (*e.g.* alveolar swelling, gingival redness).[1]

The spectrum of typical imaging findings in MRONJ include sclerosis, periosteal thickening and osteolysis, as described in numerous studies.[5–7] Panoramic radiographs, cone-beam computed tomography (CBCT) and multi detector CT are used most often as they perform best for bone depiction.[8–10] Despite advances in radiographic diagnosis of MRONJ and subtle bone changes already occurring at Stage 0,[11] patients are often not properly diagnosed using current clinical criteria. In addition, the risk of disease progression from usually undetected Stage 0 is about 50%.[6] As the diagnosis of MRONJ is currently based on clinical history and examination it is not only inaccurate, but often delayed.[12] Alternative imaging concepts for early disease recognition and extent assessment are needed in order to prevent MRONJ-associated complications.[13]

A wide spectrum of alternative imaging modalities for detection and grading of early stage MRONJ has recently been investigated by numerous authors.[14] However, the role of MRI in MRONJ diagnosis besides assessing adjacent soft tissue and ruling out possible complications,[15] has not been completely defined yet. Recently, ultra-short echo-time (UTE) MRI sequences have been proven to be of similar diagnostic accuracy compared to CBCT images for jaw bone evaluation in MRONJ patients.[9] In addition, dynamic contrast-enhanced (DCE) bone perfusion MRI could help in better assessing bone viability with better characterization of disease extent.[16] DCE-MRI in general reflects pathologic changes in microcirculation as a time dependent T1-relaxivity change with Gadolinium passing through the examined volume.[17,18] Moreover, DCE bone perfusion MRI has proven valuable in the evaluation of osteonecrosis of the patella and femur[18–20] but has not been applied to MRONJ patients so far. The rationale behind this investigation was hence to transfer current knowledge about DCE-MRI from related pathologies to MRONJ and a possible gain in knowledge especially regarding sub clinical stages.

The aim of this study was to correlate DCE-MRI bone perfusion with morphologic UTE bone imaging findings and to investigate whether DCE perfusion could serve as surrogate for dedicated bone imaging in the identification of MRONJ foci in patients.

Methods and materials

Patient population

This study was approved by the responsible local ethics committee (Cantonal Ethics Committee Zurich). Only patients with priorly obtained written informed consent were included. Over a period of 13 months, MRI scans, performed according to an institute-own protocol for MRONJ imaging, were screened. Only patients with histologically proven MRONJ according to AAOMS criteria were included.[1] The internal search was performed using the PACS system (Agfa IMPAX v. 6.7, Agfa-Gevaert N.V., Mortsel, Belgium). 19 of the 20 included patients have been previously reported.[9] This prior article dealt with the utilization of UTE-MRI for MRONJ identification and characterization, whereas in this manuscript we report on the diagnostic performance of DCE-MRI compared to the reference standard of UTE-MRI.

MR imaging

All MRIs were performed on a 3T unit (Skyra, Siemens Healthineers, Erlangen, Germany), with the patient in supine position and the head in a dedicated 64-channel head array coil (Siemens Healthineers). Imaging was performed in one session per patient. In addition to coronal T_1 weighted (W) and axial fat-saturated T_2W turbo-spin echo (TSE) sequences, functional UTE- and DCE-images were obtained. For jawbone imaging, a vendor-specific UTE-MRI sequence using pointwise encoding time reduction with radial acquisition was used ("PETRA", also Siemens Healthineers).[17] Sequence parameters for UTE-MRI were a 0.7 mm isovolumetric voxel size, 0.07 ms TE, 5 ms TR, 246 mm field of view at 315 s acquisition time. Base resolution was 352 with a bandwidth of 355 Hz/Px. For DCE imaging a T_1W 3D gradient-echo sequence ("VIBE": 0.5 × 0.5 mm in-plane voxel size, 2 mm slice thickness, TE 1.47 ms, TR 2.95 ms, 256 mm field of view, 980 Hz/Px) of the jaws was repeatedly acquired, in order to monitor bone perfusion over time (20 continuous measurements without

pausing, total acquisition time 151 s). A contrast bolus of Gadobutrol (Gadovist®, Bayer AG) 1 mmol ml^{-1} at a dosage of 0.1 ml/kg bodyweight was applied intravenously followed by a 10 ml saline flush. Only MR examinations with high-quality UTE- as well as DCE perfusion-images were used for further analysis.

Qualitative readout

The UTE-MRI were analyzed by two radiologists (R.G., F.A.H., 12 and 2 years of musculoskeletal radiology experience) independently after randomization of patients using a 4-point Likert scale (0–3, for "normal findings", "mild", "moderate" and "severe" changes) for visual hallmarks (periosteal thickening, osteolysis and bone sclerosis) typically associated with MRONJ.[6] The majority of the cohort has already been investigated by a comparison of MRONJ hallmarks in CBCT with UTE-MRI in a recently published study.[9] Due to resolution and sinus air artifact issues in DCE-MRI, only mandibular regions were assessed bilaterally: anterior corpus of mandible (aMa, *i.e.* comprised between mental foramina), posterior corpus of mandible (pMa, between mental foramen and angle of the mandible), Ramus mandibulae (rMa), condyloid process of mandible (conMa). Consensus reading was performed for discordant ratings and used as standard-of-reference for comparison with quantitative DCE-MRI perfusion data. Due to results from the preceding publication, we intentionally did not perform inter -reader agreement for this study.[9]

Quantitative readout

Quantitative readout was performed using a vendor workflow solution ("syngo.via" Module Tissue 4D, VB30A, also Siemens Healthineers). Preprocessing included calculation of perfusion maps (wash-in, wash-out, arrival time (AT), time to peak (TTP), peak enhancement intensity (PEI), initial area under the curve (iAUC)) within same-sized volumes of interest (VOI), as well as semi-rigid co-registration of perfusion with morphologic PETRA images.[21,22] Due to preceding testing of VOI-measurements at study-unrelated subjects, an arbitrarily defined size of a spherical VOI of 41 voxels (ca. 5 mm^3) was considered as optimum (*i.e.* largest possible overall without interference with adjacent structures, such as inferior alveolar nerve), and therefore used for all subsequent measurements. Region-specific VOIs were then placed in a total of six regions of the mandible (aMa, pMa and rMa bilaterally). The measurements were placed in the bone marrow with margins of several millimeters in the mandibular base to avoid measuring cortical bone. The conMa was excluded as it is very rarely affected by MRONJ, and the anatomical form of the bone marrow made consistent VOI placement impossible. To improve comparability among patients, all quantitative DCE measurements were internally referenced to the first and second cervical vertebral bodies after prior exclusion of bone metastases or other osseous pathologies. Furthermore, VOI measurements were performed in the axis body and compared with measurements of the supposedly healthy side of the jaw, in order to exclude a potential bias of disease spread into the healthy jaw regions.

In every second randomly chosen patient of the cohort quantitative readout was performed twice after a delay of 4 weeks, in order to assess measurement reproducibility using intraclass correlation coefficient (ICC) analysis.

Statistical analysis

The Mann–Whitney *U*-test was first used to compare medians for each quantitative DCE-MRI parameter (wash-in, wash-out, AT, TTP, PEI, iAUC), separately using the binarized groups "pathologic" and "non-affected" from the qualitative UTE-MRI readout. Bone regions were considered pathologic if any of the three qualitative hallmarks were graded ≥2. Each visually graded hallmark was assessed independently ("sclerosis", "periosteal thickening", "osteolysis"), again using Mann–Whitney *U*-test and the binarized scores "pathologic" and "non-affected" for each quantitative DCE-MRI parameter individually. Effect size *r* was calculated for both analyses and was interpreted according to Rosenthal and Rosnow (1984) ($r > 0.1$: small effect size; $r > 0.3$: medium effect size; $r > 0.5$: large effect size).[23] Comparisons between healthy jaw and axis body were performed in analogous fashion. Additionally, in order to test for influence of bone osteolysis on DCE parameters, pathologic regions based on binarized productive changes (periosteal thickening and/or sclerosis) with or without presence of osteolysis were compared to each other.

Receiver operating characteristic (ROC) curves were plotted for each DCE-MRI parameter individually (wash-in, PEI, iAUC), to determine the area under the curve (AUC) as measure for diagnostic performance.[24] The ROC curves were then used to determine possible cut-off values for each significant parameter at a specificity of 90% and a sensitivity of 90%, as well as Youden's J maximal value as a measure for maximal diagnostic accuracy.[25] Pearson's correlation was used to test for correlation of DCE bone perfusion parameters with age in regions classified as non-affected by MRONJ.

p-values < 0.05 were considered statistically significant for all measurements. Statistical calculations were performed using IBM SPSS Statistics (v. 25, IBM, Armonk, NY).

Results

A total of 20 patients were included in this study, 11 female and 9 male patients, between 57 and 93 years of age, with a mean of 75.9 ± 10.1 years. The patients developed MRONJ after treatment with denosumab ($n = 8$), zoledronate ($n = 3$), ibandronate ($n = 3$), denosumab/

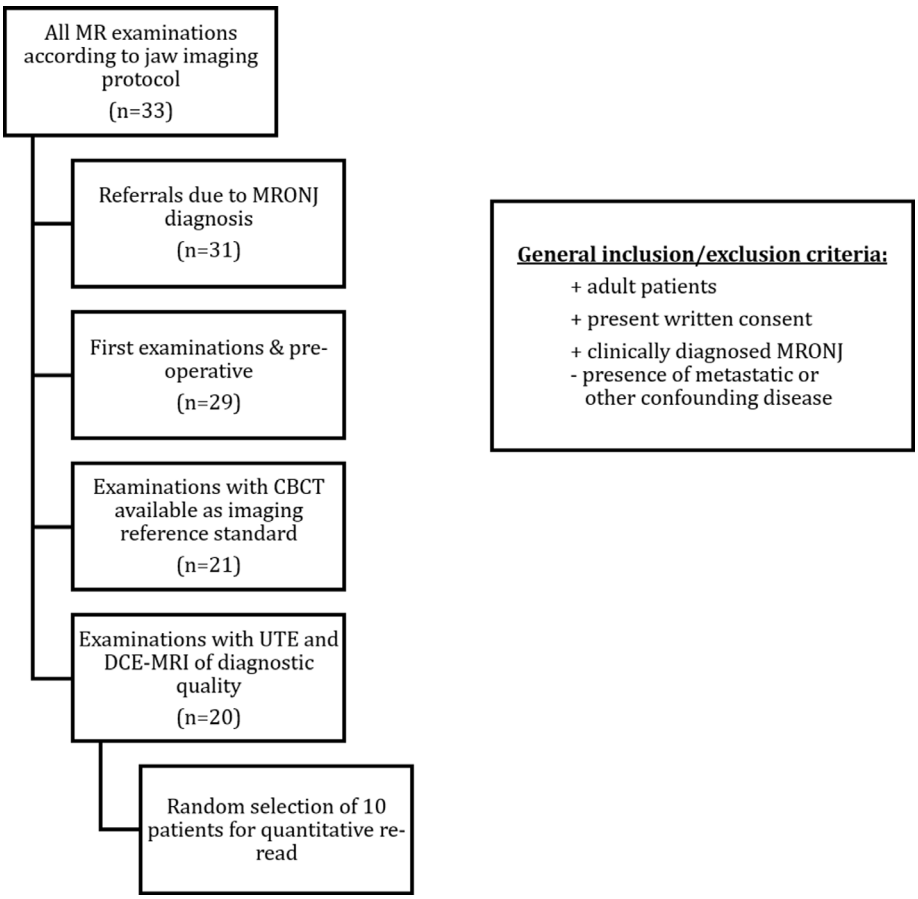

Figure 1 Flowchart of patient inclusion according to the STARD checklist. MRONJ, medication-related osteonecrosis of the jaw; UTE, ultra-short echo-time.

zoledronate (n = 2), bortezomib/cyclophosphamide (n = 1), bortezomib/zoledronate (n = 1), bortezomib/denosumab (n = 1), or denosumab/everolimus/sunitinib (n = 1). The majority of patients suffered from non-malignant disease, *i.e.* primary osteoporosis (n = 11; prostate cancer: n = 4; various malignant entities for the remainder cases). A STARD-compliant flowchart of in- and exclusion criteria is shown in Figure 1. A total 49 pathologic and 71 non-affected mandibular regions were qualitatively and quantitatively assessed in this study. The distribution of MRONJ lesions in the patient cohort within the evaluated regions of the mandible is displayed in Table 1.

Qualitative readout

41% (24 regions) of pathologic regions showed productive bone changes (*i.e.* sclerosis or periosteal thickening) without osteolysis, 59% (34 regions) showed productive changes in combination with osteolysis. Osteolysis was present only in regions with productive changes (2% (1 region): with periosteal thickening/9% (5 regions): with sclerosis/48% (28 regions): with sclerosis + periosteal thickening). Sclerosis was only present in combination with periosteal thickening (5% (3 regions): only periosteal thickening/sclerosis + periosteal thickening). All patients exhibited only one contiguous lesion, spanning one or more regions of the mandible.

Table 1 Distribution pattern of pathologic and non-affected regions (n = 49) in the mandible (aMa: anterior mandible, pMa: posterior mandible, rMa: ramus mandibularis) in total study cohort (n = 20)

	Overall	*Right aMa*	*Right pMa*	*Right rMa*	*Left rMa*	*Left pMa*	*Left aMa*
Pathologic	49	11 (55%)	11 (55%)	9 (45%)	3 (15%)	6 (30%)	9 (45%)
PC w/out osteolysis	23	5	5	7	1	1	4
PC with osteolysis	26	6	6	2	2	5	5
Non-affected	71	9	9	11	17	14	11

Numbers are displayed for regions with productive changes (PC; periosteal thickening and/or sclerosis) with and without osteolysis, respectively.

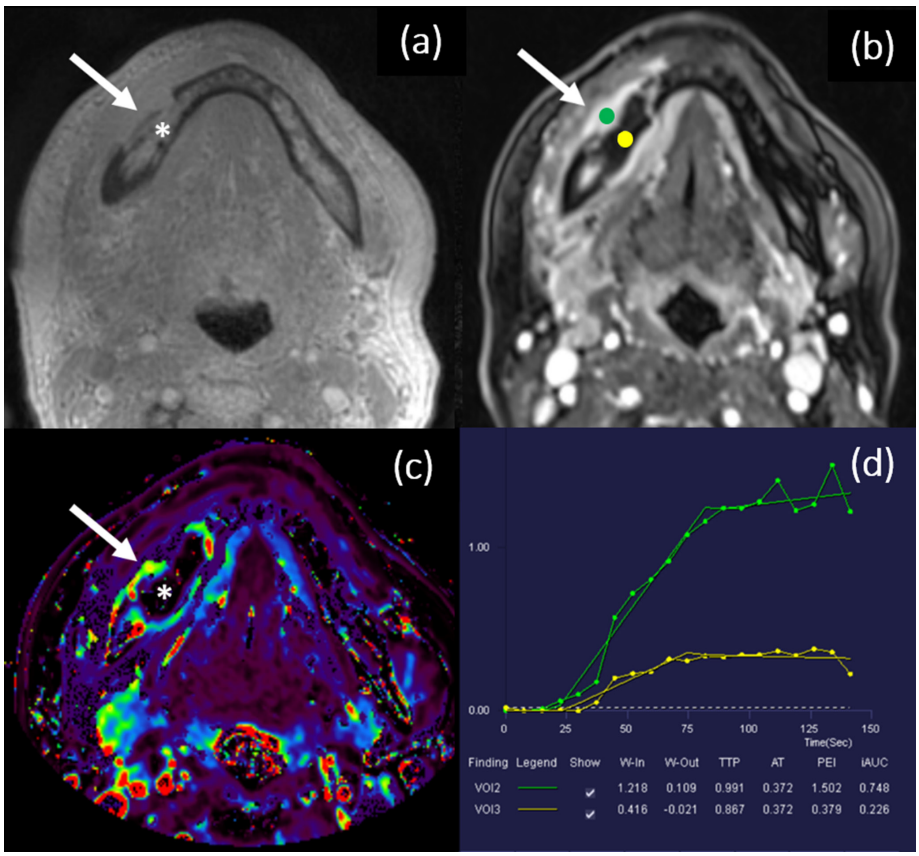

Figure 2 MRONJ focus (asterisk) with periosteal thickening in right anterior and posterior mandible, but also bone fragmentation and osteolysis (arrow) in right posterior mandible on UTE image (a). On late phase of a T_1W fat-saturated DCE image (b) surrounding hyperperfusion can be seen (arrow) around the necrotic area. On iAUC perfusion map (c) increased values (green pixels) are seen in areas surrounding necrosis, compared to contralateral normal healthy bone (dark and blue pixels). Respective VOI placements in necrotic (VOI 3, yellow) and perifocal hyperemic bone (VOI 2, green) confirm increased perfusion in both MRONJ-affected core and surrounding area (d), corroborating inflammatory hyperperfusion of necrotic bone. DCE, dynamic contrast enhanced; iAUC, initial area under the curve; MRONJ, medication-related osteonecrosis of the jaw; UTE, ultra-short echo-time; VOI, volume of interest

Quantitative readout

DCE bone perfusion measurement reproducibility: All tested quantitative DCE bone perfusion MR parameters showed good reproducibility between the two readouts with ICCs ranging from 0.739 to 0.774 (wash in: 0.774, 95%CI 0.628–0.862, PEI: 0.739, 95%CI 0.570–0.842 and iAUC: 0.754, 95%CI 0.595–0.851). A representative example of relevant workflow steps is shown in Figure 2.

DCE bone perfusion correlation with imaging hallmarks: Median wash-in, PEI, and iAUC were significantly higher in pathologic compared to non-affected regions with medium to large effect sizes (Mann–Whitney $U_{\text{Wash-In}} = 1060$, $p < 0.05$, $r = 0.33$; Mann–Whitney $U_{\text{PEI}} = 735$, $p < 0.05$, $r = 0.49$; Mann–Whitney $U_{\text{iAUC}} = 700$, $p < 0.05$, $r = 0.51$), as illustrated in Figure 3. The parameters AT, wash-out and TTP did not show significant differences and were thus excluded from further analysis.

Median wash-in, PEI and iAUC were significantly higher in pathologic groups (Figure 4) with medium to large effect sizes for each individual qualitative hallmark. The binomial rating scale was again used to classify regions as "with osteolysis" *vs* "without osteolysis"; " with sclerosis" *vs* " without sclerosis" and "with periosteal thickening" *vs* "without periosteal thickening" (sclerosis: wash-in $r = 0.36$, PEI $r = 0.52$, iAUC $r = 0.54$); (periosteal thickening: wash-in $r = 0.27$, PEI $r = 0.5$, iAUC $r = 0.5$); (osteolysis: wash-in $r = 0.21$, PEI $r = 0.4$, iAUC $r = 0.43$). No significant differences were found between different imaging hallmarks (Table 2). Median wash-in, PEI and iAUC did not differ significantly between regions with productive changes with and those without osteolysis ($p_{\text{Wash-In}} = 0.535$, $p_{\text{PEI}} = 0.180$, $p_{\text{iAUC}} = 0.389$).

There were no significant differences between DCE measurements of healthy jaw regions and the axis body (all $p > 0.05$).

ROC analysis: The AUC in the ROC analysis for the DCE parameters in order to detect MRONJ affected regions were fair (wash-in: 0.626 AUC, PEI: 0.727 AUC, iAUC 0.727 AUC; Figure 5). Possible cut-off values for 90% sensitivity and specificity respectively were 0.34 and

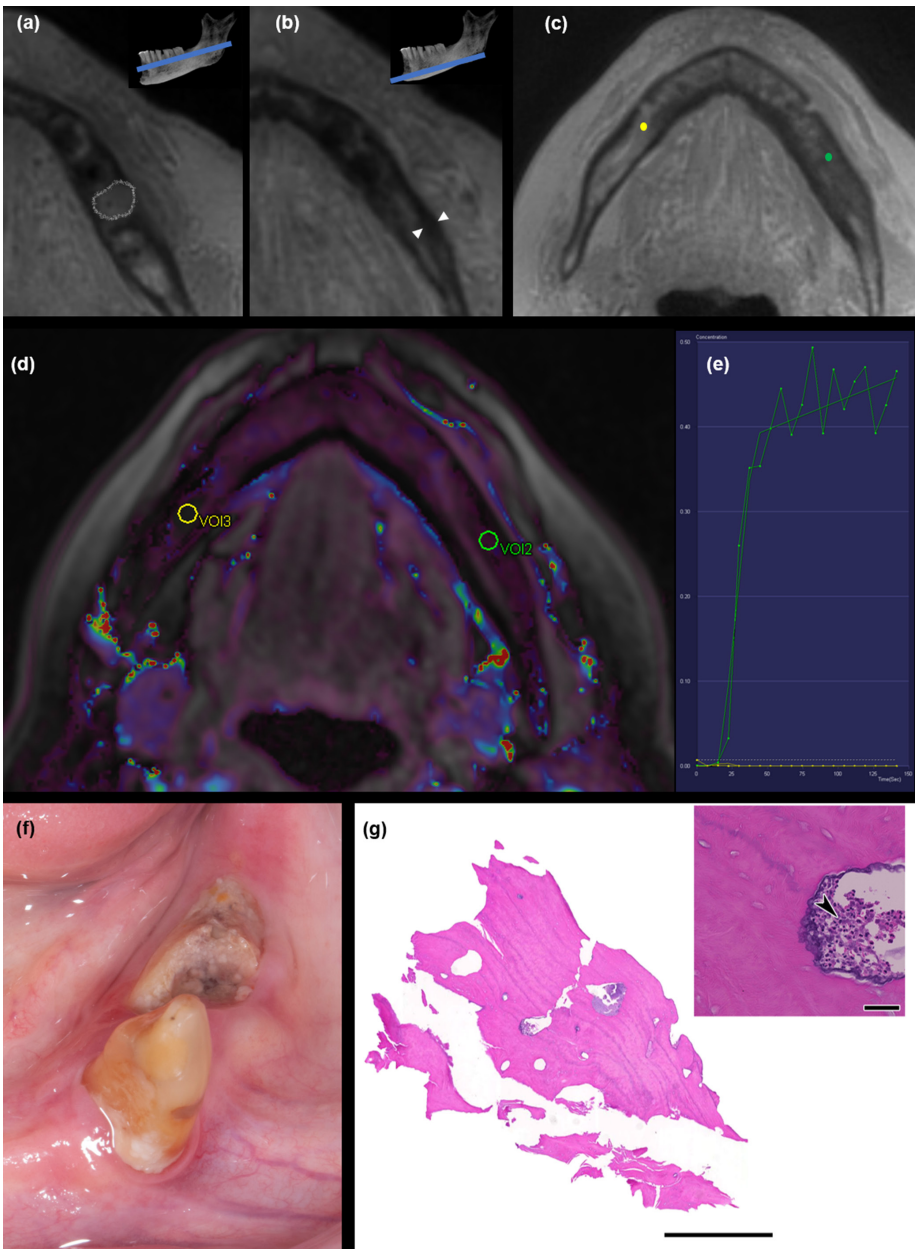

Figure 3 UTE MR images of MRONJ in left posterior mandible corpus region at (a) alveolar socket level and at (b) the base of the mandible with productive bone sclerosis and periosteal thickening (arrowheads in b) and small osteolysis on alveolar ridge (circle in a). VOIs were placed at the base of the mandible in MRONJ focus (VOI 2, green) and contralateral non-affected area (VOI 3, yellow) as shown on UTE (c) and iAUC map (d). In consecutive perfusion curves (e) markedly increased perfusion in MRONJ focus is seen, while in non-affected region a flat trajectory is seen, indicating normal minimally perfused bone. Findings illustrate increased perfusion of base in MRONJ area despite presence of apical osteolysis on UTE image. Pre-operative clinical findings are concordant showing (f) necrotic bone exposed to the oral cavity in the left posterior mandible corpus region. Post-operative histology specimens (g) identified necrotic bone and acute inflammation (overview). The inset shows H&E staining depicting avital bone featuring empty lacunae lacking osteocytes and abundant neutrophilic granulocytes attacking the bone matrix (arrowhead); scale bars 1 mm (overview) and 50 µm (insets). DCE, dynamic contrast enhanced; H&E, hematoxylin & eosin; iAUC, initial area under the curve; MRONJ, medication-related osteonecrosis of the jaw; UTE, ultra-short echo-time; VOI, volume of interest

0.248 for iAUC, 0.313 and 0.188 for PEI, −0.027 and 0.148 for wash-in. Youden's index (J) (assumption of equal importance of specificity and sensitivity) was determined for each parameter respectively and were 0.183 for iAUC, 0.326 for PEI and 0.112 for wash-in. Pearson's correlation of wash-in, PEI, iAUC with patients age in "healthy" regions showed weak ($r > 0.3$) to no ($r < 0.3$) correlation (Age: $r_{Wash\text{-}In} = 0.17$, $r_{PEI} = 0.34$, $r_{iAUC} = 0.35$).

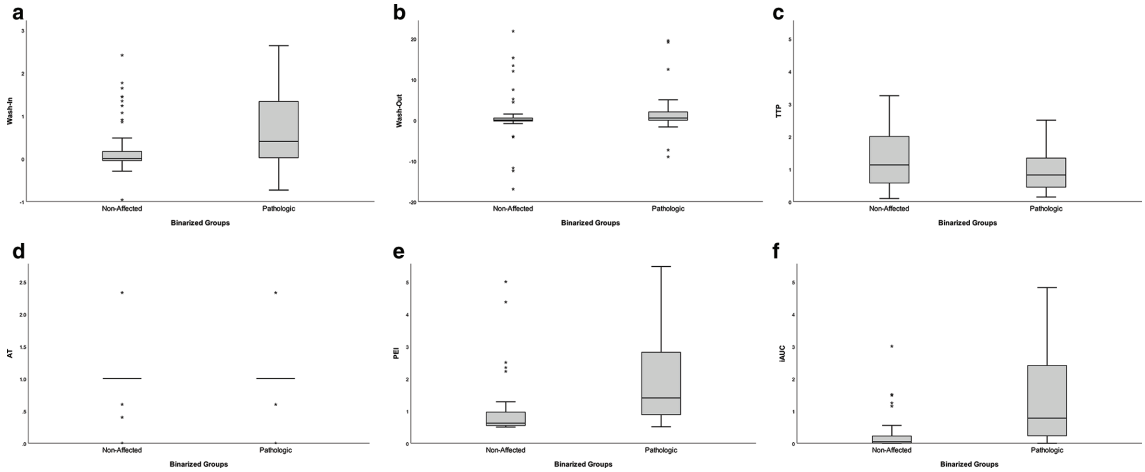

Figure 4 Boxplots displaying differences for DCE parameteres wash-in (a), wash-out (b), TTP(c), AT (d), PEI (e), and iAUC(f), binarized into "non-affected" and "pathologic" groups based on marked presence (Likert score 2–3) of either qualitative imaging hallmark (osteolysis, bone sclerosis or periostal thickening), respectively. Signficant differences between groups were found for wash-in, PEI and iAUC (all $p < 0.01$). AT, arrival time; DCE, dynamic contrast enhanced; iAUC, initial area under the curve; PEI, peak enhancement intensity; TTP, time to peak

Discussion

As mere clinical assessment only detects overt MRONJ foci and often underestimates the extent of the disease radiologic assessment is becoming more important for timely and accurate diagnosis and therapy planning.[13] In addition to information on bone morphology, functional MRI, *e.g*. bone perfusion studies can also look at vascular integrity of bone tissue and offer new perspectives on disease assessment. This study aimed to demonstrate the ability of DCE-MRI bone perfusion imaging to serve as surrogate for morphologic UTE-MRI bone imaging in distinguishing pathologic from healthy bone regions in the mandible using histology proven MRONJ as standard of reference.

Significant differences for perfusion parameters were found when testing for different morphologic hallmarks ("sclerosis", "periosteal thickening", "osteolysis"), without significant differences among them. This suggests that there may be no single dominant imaging hallmark of MRONJ with regard to impact on perfusion changes and also illustrates the complex and heterogenous morphologic appearance with simultaneous productive and lytic changes of these lesions.

All hallmarks were present in necrotic jawbone areas with productive changes seemingly preceding osteolysis. The latter was only present in regions with at least one other productive change. We also investigated the significance of osteolysis as a purportedly specific morphologic imaging surrogate for relevant bone necrosis on perfusion behavior. Interestingly, no statistical difference was seen between MRONJ regions with productive changes only (sclerosis and/or periosteal thickening) and those with osteolysis, even though osteolytic or necrotic bone would be expected to show decreased perfusion. This may be explained first in part by VOI placements at the mandibular base distant to the alveolar process and the periodontal interface where MRONJ is usually thought to initiate.[1] Thus, mere osteolytic bone may not have been included in the VOI and the measurements may reflect predominately productive changes bordering the osteolytic process. Secondly, a number of studies have presented contradictory results on the relationship of DCE bone perfusion MRI with osteonecrosis and in particular osteolysis in other regions of the body or other disease entities such as Kienböck's disease and scaphoid non-union fractures.[26,27] These studies suggest increased perfusion in osteolytic regions when compared to healthy bone while also showing decreased perfusion in later stages of osteonecrosis. Hence, based on the current literature the correlation of qualitative bone changes and bone viability in osteonecrotic patients with quantitative DCE-MRI parameters remains unclear.[27]

In this study cohort perfusion parameters wash-in, PEI, iAUC showed significantly higher median values in pathologic regions than in healthy jawbone, despite

Table 2 Quantitative DCE parameters separately for different hallmarks

	Sclerosis		*Periosteal thickening*		*Osteolysis*	
Wash-in	p	<0.05	p	<0.05	p	<0.05
	r	0.36	r	0.27	r	0.21
PEI	p	<0.05	p	<0.05	p	<0.05
	r	0.52	r	0.5	r	0.4
iAUC	p	<0.05	p	<0.05	p	<0.05
	r	0.54	r	0.5	r	0.43

PEI, peak enhancement intensity; iAUC, initial area under the curve. Values represent *p*-values (p) and effect sizes (r) of Mann–Whitney *U* Test. The differences between hallmarks were almost negligible. Wash-in, PEI and iAUC, which were all significantly different between non-affected and pathologic regions (refer to Table 2), showed comparable effect sizes (r) among different qualitative hallmarks (sclerosis, periosteal thickening or osteolysis) used for binarization into pathologic *vs* non-affected lesions

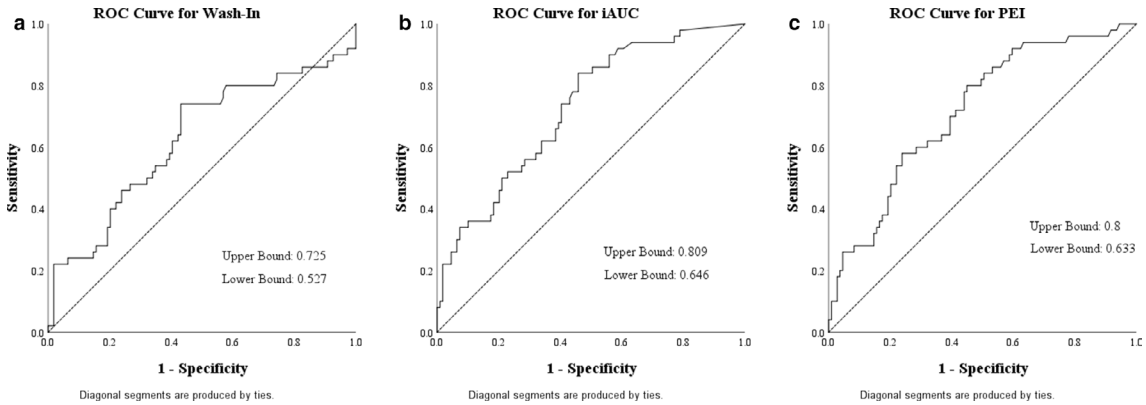

Figure 5 ROC curves for (a) wash-In, (b) iAUC and (c) PEI demonstrate comparable accuracy for identification of pathologic and non-affected MRONJ regions based on binarized Likert scores (2 or 3) of either qualitative imaging hallmark (osteolysis, bone sclerosis or periostal thickening). iAUC, initial area under the curve; MRONJ, medication-related osteonecrosis of the jaw; PEI, peak enhancement intensity; ROC, receiver operating characteristic.

substantial overlap as illustrated in Figure 4. However, significant median perfusion differences were irrespective of predominant qualitative imaging hallmark. This finding is concordant with regional hyperperfusion and has also previously been reported in a study correlating imaging with histopathological findings in MRONJ, describing areas of diseased unexposed bone with hypervascular fibrous tissue and inflammatory infiltrate filling intertrabecular spaces.[28]

Increased T_1 signal in DCE bone perfusion MRI is dependent on the tissue blood flow (intravascular gadolinium) as well as the permeability of the blood vessels leading to increased extravascular volume fraction (gadolinium in the extravascular space).[17] Our findings of hyperperfusion are most likely caused by a combination of both effects induced by inflammatory reaction in the jawbone. In a study of osteonecrosis of the femoral head correlating histopathological specimens with DCE perfusion MRI Chan et al[19] postulate, that gadolinium enhancement is mostly due to inflammatory infiltrates, fibrocytic repair and viable granulation tissue surrounding necrotic bone areas. MRONJ shows histomorphologic similarities with usually abundant inflammatory cell infiltrates in addition to necrotic bone areas.[29]

In their study, Chan et al also propose a trend of decreased blood perfusion, but increased blood pressure within the affected area, to explain perfusion MRI results with higher peak signal intensities in osteonecrotic regions of the hip.[19] This hypothesis could also be transferred to our findings. Clinically, hypervascularity or hyperemia in early stages of MRONJ could lead to an increase in intramedullary pressure, which could explain symptoms (*e.g.* odontalgia, dull aching bone pain) patients experience in earlier stages of the disease (Stage 0 non-exposed variant).

ROC curve analysis of DCE parameters were based on dichotomized qualitative ratings and revealed AUC values ranging from 0.626 to 0.727 with overall fair diagnostic performance for detection of MRONJ associated bone changes due to certain overlap of perfusion parameters in healthy *vs* pathologic jaw bone regions. Hence, DCE imaging at present cannot be regarded as a fully valid substitute to UTE or CBCT images for MRONJ identification but they could potentially increase reader confidence when added to traditional morphologic TSE MR sequences of the jaw. Subsequently, DCE may be a useful additive in fully MRI-based diagnostic decision making for MRONJ, potentially allowing for radiation-free imaging workflows for this disease entity in the future. Despite the usually higher age of typical MRONJ patients, it should be kept in mind that those patients usually carry long medical histories with rather high cumulative radiation doses. On the other hand, issues of gadolinium retention in the brain should be considered, especially ensuring to exclude renal impairment and to use macrocyclic gadolinium-based contrast agents. Perfusion changes measured by DCE MRI might help in revealing MRONJ Stage 0 with alterations present at a cellular or histopathological level, but invisible to the human eye by means of qualitative imaging or clinical inspection. A possible approach would be further investigation of jaw perfusion in imaging, *e.g.* using an animal model, correlated to a 3D histopathologic segmentation as the reference standard.

There are several limitations to this study. First, perfusion parameters were correlated with qualitative morphologic bone changes in UTE imaging. Despite histologic confirmation of MRONJ lesions, known heterogeneity of jawbone within small disease foci may impact on DCE perfusion behavior. Secondly, although UTE images have been shown to perform comparably well compared to CBCT,[9] the latter is still considered the gold-standard for jawbone imaging. However, due to results of a previous investigation, we assumed excellent comparability between the two modalities UTE and CBCT. Hence, we decided to choose a reference standard that allows for assessment without need for atlas co-registration and potential biases due to differences between two examination dates, as all examinations of this

study were performed in one session per patient. Third, morphologic bone changes do not depict true extent of diseased bone in MRONJ and there is no consensus on which hallmark is the most important with regard to disease extent. Moreover, it has to be mentioned, that potentially missed lesions that were considered as "non-affected" in UTE can lead to biased results. However, surgical resection borders were known to be "healthy" in all patients, and we considered multifocal appearance as unlikely. Additionally, comparison of healthy regions with the distant axis bone showed no significant differences, which also indicates the observation of true healthy regions. Due to ethical concerns, comparison of DCE-MRI from healthy volunteers was not performed. Fourth, the predictive value of MR perfusion for histologic bone vitality/necrosis was not assessed in this study. Further radiopathologic correlation studies are needed and may reveal significantly larger disease extent than is currently being detected by clinical findings and qualitative grading in clinical imaging in MRONJ patients.

Conclusion

In conclusion, despite significant overlap of perfusion data among healthy and diseased jawbone DCE bone perfusion MRI shows significant correlation with morphologic changes on UTE-MRI bone images in patients with MRONJ. Although it cannot be regarded as a fully valid substitute to UTE or CBCT images for MRONJ identification it may nevertheless enhance reader confidence and treatment planning in MRONJ patients.

Funding

This research did not receive any specific grant from funding agencies in the public, commercial, or not-for-profit sectors.

REFERENCES

1. Ruggiero SL, Dodson TB, Fantasia J, Goodday R, Aghaloo T, Mehrotra B, et al. American Association of Oral and Maxillofacial Surgeons position paper on medication-related osteonecrosis of the jaw--2014 update. *J Oral Maxillofac Surg* 2014; **72**: 1938–56. doi: https://doi.org/10.1016/j.joms.2014.04.031
2. Lin JH. Bisphosphonates: a review of their pharmacokinetic properties. *Bone* 1996; **18**: 75–85. doi: https://doi.org/10.1016/8756-3282(95)00445-9
3. Ikebe T. Pathophysiology of BRONJ: drug-related osteoclastic disease of the jaw. *Oral Sci Int* 2013; **10**: 1–8. doi: https://doi.org/10.1016/S1348-8643(12)00045-6
4. Aghaloo T, Hazboun R, Tetradis S. Pathophysiology of osteonecrosis of the jaws. *Oral Maxillofac Surg Clin North Am* 2015; **27**: 489–96. doi: https://doi.org/10.1016/j.coms.2015.06.001
5. Phal PM, Myall RWT, Assael LA, Weissman JL. Imaging findings of Bisphosphonate-associated osteonecrosis of the jaws. *AJNR Am J Neuroradiol* 2007; **28**: 1139–45. doi: https://doi.org/10.3174/ajnr.A0518
6. Cardoso CL, Barros CA, Curra C, Fernandes LMPdaSR, Franzolin SdeOB, Júnior JSF. Radiographic findings in patients with medication-related osteonecrosis of the jaw. *Int J Dent* 2017; **2017**: 1–6. doi: https://doi.org/10.1155/2017/3190301
7. Guggenberger R, Koral E, Zemann W, Jacobsen C, Andreisek G, Metzler P. Cone beam computed tomography for diagnosis of bisphosphonate-related osteonecrosis of the jaw: evaluation of quantitative and qualitative image parameters. *Skeletal Radiol* 2014; **43**: 1669–78. doi: https://doi.org/10.1007/s00256-014-1951-1
8. Berg B-I, Mueller AA, Augello M, Berg S, Jaquiéry C. Imaging in patients with Bisphosphonate-associated osteonecrosis of the jaws (MRONJ. *Dent J* 2016; **4**: E29: 29: 02 Sep 2016. doi: https://doi.org/10.3390/dj4030029
9. Huber FA, Schumann P, von Spiczak J, Wurnig MC, Klarhöfer M, Finkenstaedt T, et al. Medication-Related osteonecrosis of the Jaw-Comparison of bone imaging using ultrashort Echo-Time magnetic resonance imaging and cone-beam computed tomography. *Invest Radiol* 2020; **55**: 160–7. doi: https://doi.org/10.1097/RLI.0000000000000617
10. Kälin PS, Huber FA, Hamie QM, Issler LS, Farshad-Amacker NA, Ulbrich EJ, et al. Quantitative MRI of visually intact rotator cuff muscles by multiecho Dixon-based fat quantification and diffusion tensor imaging. *J Magn Reson Imaging* 2019; **49**: 109–17. doi: https://doi.org/10.1002/jmri.26223
11. Soundia A, Hadaya D, Mallya SM, Aghaloo TL, Tetradis S. Radiographic predictors of bone exposure in patients with stage 0 medication-related osteonecrosis of the jaws. *Oral Surg Oral Med Oral Pathol Oral Radiol* 2018; **126**: 537–44. doi: https://doi.org/10.1016/j.oooo.2018.08.005
12. Assili Z, Dolivet G, Salleron J, Griffaton-Tallandier C, Egloff-Juras C, Phulpin B. A comparison of the clinical and radiological extent of denosumab (Xgeva. *J Clin Med* 2021; **10**.
13. Schiodt M, Otto S, Fedele S, Bedogni A, Nicolatou-Galitis O, Guggenberger R, et al. Workshop of European Task force on medication-related osteonecrosis of the jaw-Current challenges. *Oral Dis* 2019; **25**: 1815–21. doi: https://doi.org/10.1111/odi.13160
14. Wongratwanich P, Shimabukuro K, Konishi M, Nagasaki T, Ohtsuka M, Suei Y, et al. Do various imaging modalities provide potential early detection and diagnosis of medication-related osteonecrosis of the jaw? A review. *Dentomaxillofac Radiol* 2021; **20200417**: 20200417. doi: https://doi.org/10.1259/dmfr.20200417
15. Morag Y, Morag-Hezroni M, Jamadar DA, Ward BB, Jacobson JA, Zwetchkenbaum SR, et al. Bisphosphonate-Related osteonecrosis of the jaw: a pictorial review. *Radiographics* 2009; **29**: 1971–84. doi: https://doi.org/10.1148/rg.297095050
16. Marx RE, Pamidronate MRE. Pamidronate (Aredia) and zoledronate (Zometa) induced avascular necrosis of the jaws: a growing epidemic. *J Oral Maxillofac Surg* 2003; **61**: 1115–7. doi: https://doi.org/10.1016/s0278-2391(03)00720-1
17. Cuenod CA, Balvay D. Perfusion and vascular permeability: basic concepts and measurement in DCE-CT and DCE-MRI. *Diagn Interv Imaging* 2013; **94**: 1187–204. doi: https://doi.org/10.1016/j.diii.2013.10.010
18. Lee JH, Dyke JP, Ballon D, Ciombor DM, Tung G, Aaron RK. Assessment of bone perfusion with contrast-enhanced magnetic resonance imaging. *Orthop Clin North Am* 2009; **40**: 249–57. doi: https://doi.org/10.1016/j.ocl.2008.12.003
19. Chan WP, Liu Y-J, Huang G-S, Lin M-F, Huang S, Chang Y-C, et al. Relationship of idiopathic osteonecrosis of the femoral head to perfusion changes in the proximal femur by dynamic contrast-enhanced MRI. *AJR Am J Roentgenol* 2011; **196**: 637–43. doi: https://doi.org/10.2214/AJR.10.4322

20. van der Heijden RA, Poot DHJ, Ekinci M, Kotek G, van Veldhoven PLJ, Klein S, et al. Blood perfusion of Patellar bone measured by dynamic contrast-enhanced MRI in patients with patellofemoral pain: a case-control study. *J Magn Reson Imaging* 2018; **48**: 1344–50. doi: https://doi.org/10.1002/jmri.26174
21. Jahng G-H, Li K-L, Ostergaard L, Calamante F. Perfusion magnetic resonance imaging: a comprehensive update on principles and techniques. *Korean J Radiol* 2014; **15**: 554–77. doi: https://doi.org/10.3348/kjr.2014.15.5.554
22. Gordon Y, Partovi S, Müller-Eschner M, Amarteifio E, Bäuerle T, Weber M-A, et al. Dynamic contrast-enhanced magnetic resonance imaging: fundamentals and application to the evaluation of the peripheral perfusion. *Cardiovasc Diagn Ther* 2014; **4**: 147–64. doi: https://doi.org/10.3978/j.issn.2223-3652.2014.03.01
23. Rosenthal R. Effect sizes: Pearson's correlation, its display via the BESD, and alternative indices. *American Psychologist* 1991; **46**: 1086–7. doi: https://doi.org/10.1037/0003-066X.46.10.1086
24. Hajian-Tilaki K, Characteristic RO. Roc) curve analysis for medical diagnostic test evaluation. *Caspian journal of internal medicine* 2013; **4**: 627–35.
25. Youden WJ. Index for rating diagnostic tests. *Cancer* 1950; **3**: 32–5. doi: https://doi.org/10.1002/1097-0142(1950)3:1<32::AID-CNCR2820030106>3.0.CO;2-3
26. Donati OF, Zanetti M, Nagy L, Bode B, Schweizer A, Pfirrmann CWA. Is dynamic gadolinium enhancement needed in MR imaging for the preoperative assessment of scaphoidal viability in patients with scaphoid nonunion? *Radiology* 2011; **260**: 808–16. doi: https://doi.org/10.1148/radiol.11110125
27. Müller G, Månsson S, Müller MF, Johansson M, Björkman A. Increased perfusion in dynamic gadolinium-enhanced MRI correlates with areas of bone repair and of bone necrosis in patients with Kienböck's disease. *J Magn Reson Imaging* 2019; **50**: 481–9. doi: https://doi.org/10.1002/jmri.26573
28. Bedogni A, Blandamura S, Lokmic Z, Palumbo C, Ragazzo M, Ferrari F, et al. Bisphosphonate-Associated jawbone osteonecrosis: a correlation between imaging techniques and histopathology. *Oral Surg Oral Med Oral Pathol Oral Radiol Endod* 2008; **105**: 358–64. doi: https://doi.org/10.1016/j.tripleo.2007.08.040
29. Hansen T, Kunkel M, Weber A, James Kirkpatrick C. Osteonecrosis of the jaws in patients treated with bisphosphonates - histomorphologic analysis in comparison with infected osteoradionecrosis. *J Oral Pathol Med* 2006; **35**: 155–60. doi: https://doi.org/10.1111/j.1600-0714.2006.00391.x